

# NUMERICAL MODELING OF THE TIME DEPENDENT DEGRADATION OF THE MECHANICAL PROPERTIES OF A METRO UNDERGROUND GALLERY

Taous Kamel<sup>1</sup>, Frédéric Pellet<sup>1</sup>, Claire Silvani<sup>1</sup> and Patrick Goirand<sup>2</sup>

<sup>1</sup> INSA – Laboratory of Civil and Environmental Engineering, University of Lyon, France

<sup>2</sup> RATP- Paris, France

## ABSTRACT

Several weathering factors affect tunnels by inducing a loss of strength properties of the lining support. This paper reports a study of a gallery of the Parisian metro in which cracks have been developed in the lining support due to the deterioration of the materials in the abutment. A particular attention is paid to the determination of the initial state of stresses applied on the structure right after the construction. A numerical study is then presented to simulate strain softening and the evolution over time of the underground structure. The numerical modeling is carried out using a time dependent constitutive law that takes into account the viscoplastic behavior in the lining support. The results are in accordance with the damaged areas observed in situ, particularly in terms of location of cracking. It is planned in the future to extend this approach by applying it to other cases of underground galleries.

## KEYWORDS

Tunnels, degradation, strain softening, viscoplastic behaviour, finite element, time dependent.

## INTRODUCTION

Weathering may be defined as the chemical or physical alteration of building material like rock, masonry and mortar at its surface by its reaction with aqueous and atmospheric gas solutions. The engineering interest in weathering arises because of its influence on the mechanical properties of the intact material. The underground weathering processes are chiefly chemical in origin. These include dissolution, oxidation and hydration. Some weathering actions are readily appreciated, such as the dissolution of limestone in an altered groundwater environment, or a reduction in others materials like a softening of marl due to sulphate removal. In others, such as the oxidation of mortar, the susceptibility of some forms of the mineral to rapid chemical attack is not fully understood. This discussion does not identify all of the unique issues to be considered in material degradation.

The tunnels of Paris metro are among the structure degraded under the meteoric water or wastewater infiltrations and the absorption of atmospheric carbon dioxide. These factors lead to the physical and chemical transformation in the original structure and create a deep or superficial weathering in the tunnel lining like: increase of porosity, cracks and dissolution. It appears that weathering causes a steady reduction in material properties.

In the literature, various degradation processes may affect materials (rock, masonry, mortar) and structures (tunnel, etc.). They are studied by different methods. Some researchers proceeded to model the degradation by taking into account the chemical weathering: Ryu and al. (2002), found that compressive strength decreases with the increase in the diffusion conversion period by considering that the degradation of mortar can be caused by calcium leaching due to on-site water; Fernandez-Merodo and al. (2007) opted for an approach based on establishing an index of degree of alteration  $X_d$ , this parameter represents a macroscopic measurement of the effect of external agents

(physical and chemical) on the mechanical behavior of the material (chemo-mechanical coupling); Torrenti and al. (2008), coupled leaching and creep of concrete.

Others analyzed and modeled the effect of degradation processes on the mechanical properties: Kasim and Shakoor (1996), investigated the relationship between uniaxial compressive strength and degradation for selected rock types (limestone, sandstones), by using regression analyses to determine whether degradation was a useful predictor of compressive strength. According to Xie and al. (2011), it is found that the chemical degradation induces the diminution of elastic modulus and material cohesion.

Ladanyi (1974) modeled the alteration by a reduction of strength properties with time, using a hyperbolic law. However, in this approach, only two characteristic limits were considered, a short-term and a long term. Later Ladanyi (1980) refined his study and assumed that the rock mass around the tunnel creeps according to a non-linear Maxwell (power law) model. In 1988, Ladanyi and Gill proposed a study from the convergence-confinement method modified to take into account aging. The same principle was adopted by Sandrone and Labiouse (2009). Idris and al. (2008, 2009) modeled the instability problems in tunnels due to aging phenomena on both blocks and mortars by studying the influence of their mechanical properties on the tunnel. More complex behavior of viscoplastic type damageable or strain-rate softening was also implemented by other authors (Wang and al. 1997, Boidy and al. 2002, Pellet and al. 2005, 2009 and Pellet 2009).

The aim of this work is to propose a model capable to simulate behavior of the ageing and degradations effect on galleries of Paris metro. Because the tunnels were not instrumented during their construction, the initial stress state is unknown. In order to approach this initial stress state which corresponds to the construction phase of underground structures, we propose a methodology based on comparing the numerical model with analytical methods taken from literature. Then we compare 2D and 3D numerical models. The influence of mechanical parameters of soil in the initial state of stresses is also studied. Afterward, we present a study of an underground gallery in degraded state. The degradation is, in a first step, taken into account by creating void at abutment of the model. Subsequently, the behavior of the tunnel lining is described by an elastoplastic model (Drucker-Prager criterion) with strain softening associated to a viscoplastic law to take into account the deformation over time.

## DETERMINATION OF THE INITIAL STRESS STATE

In this section, an access corridor of Pasteur station is studied. The lining support of the gallery was consisted by limestone and millstone block paired with a mortar and concrete in roof. The abutment was composed by mixture of limestone, millstone and concrete or mortar. In spite of this heterogeneity, the gallery lining is considered such a homogeneous model. Therefore, the difficulty lies in the choice of mechanical properties to represent homogeneous equivalent model.

To define the initial stress state, we propose both an analytical method based on limit analysis and a numerical modeling based on the finite element method. The soil, in which the gallery is excavated, consists in a layer of marl and weak stones. Table 1 shows the properties of soil and the masonry obtained from the characterization tests. The gallery is designed at 3.2 meters deep with 3 meters of opening width.

*Table 1. Physical and mechanical properties of soil and masonry*

Material	$\rho$ (kg/m <sup>3</sup> )	E (MPa)	$\nu$	c (kPa)	$\phi$ (°)	$\psi$ (°)
Soil	2000	250	0.3	20	30	20
Masonry lining	2400	3200	0.3	2850	30	0

*Comparison of analytical and 2D numerical approaches*

First, the pressure to be applied by the ground support to ensure the stability of the gallery is computed by a finite element calculation. Then this result is compared to those obtained from analytical approaches like Terzaghi method of (1943), that takes into account the shape of the tunnel (rectangular or circular), and the static approach of Caquot (Caquot and Kerisel 1966). Analytical methods are restricted as they provide upper and lower bounds of the problem. Numerical methods are more comprehensive because they allow getting more information about the fields of stress and strain.

The Finite Element code (Abaqus) was used to perform numerical model in two dimensions. In the initial state, the gallery is in a geostatic stress state. Soil and masonry are modeled with an elastic perfectly plastic constitutive model (Mohr-Coulomb failure criterion). The numerical results are expressed in terms of equilibrium stress and confinement loss (Panet 1995).

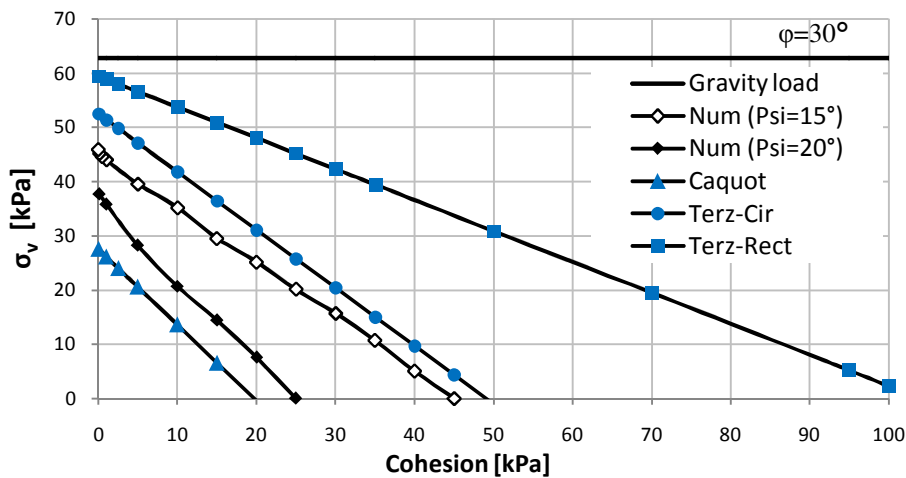


Figure 1. Equilibrium stress as a function of cohesion calculated by different approaches

Figure 1 shows the evolution of the equilibrium stress in terms of cohesion  $c$  for two values of the dilatancy angle ( $15^\circ$  and  $20^\circ$ ). This equilibrium pressure decreases with increasing cohesion. The numerical result is well supported by the analytical solutions of Caquot and Terzaghi. Note also that according to Caquot, this gallery is stable for cohesion greater or equal to 20 kPa.

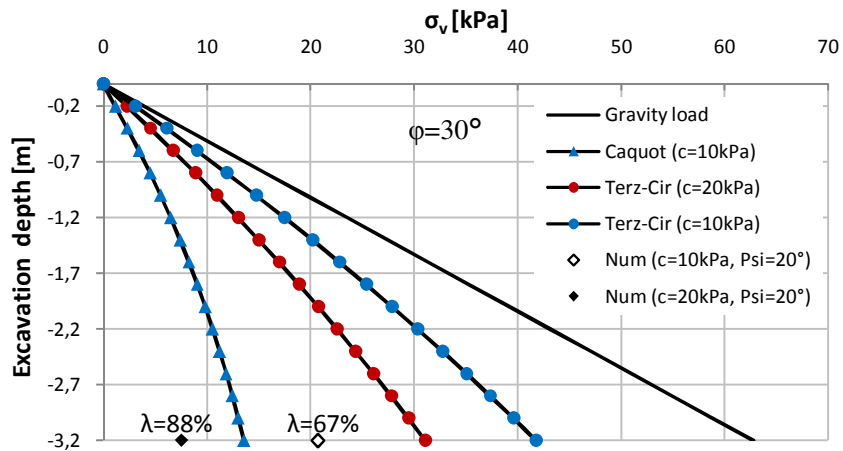


Figure 2. Equilibrium stress as a function of the depth of the excavation for two values of cohesion

The evolution of the equilibrium stress acting on the masonry lining as a function of the excavation depth was calculated with the analytical methods and finite element as shown in figure 2. The

numerical values plotted on the figure correspond to the confinement loss limit for two values of cohesion.

*Numerical comparison between 2D and 3D*

Using the convergence-confinement method (González-Nicieza and al. 2008) in 2D numerical simulations allows taking into consideration the third dimension which corresponds to the progress of the excavation. However, the confinement loss factor  $\lambda$  must be chosen carefully in order to represent correctly the initial stress state in the lining. The objective of this part is to determine the confinement loss factor  $\lambda$  from tridimensional numerical model. The confinement loss factor  $\lambda = 1 - P_i/P_0$  is between 0 and 1,  $P$  is the internal tunnel stress and  $P_0$  is the initial stress in the ground.

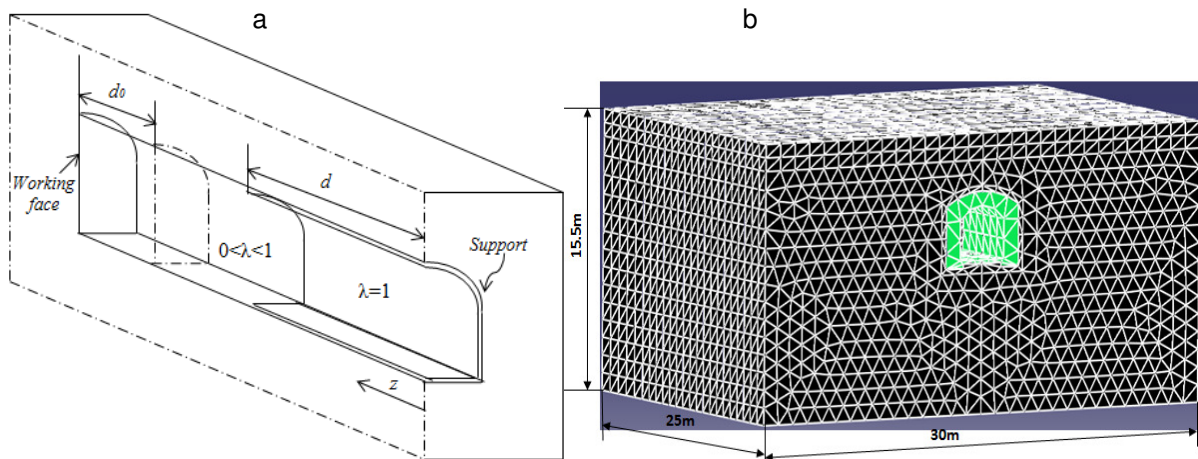


Figure 3. a. Progress of the excavation, b. Geometry and mesh of the gallery in 3D

Figure 3.a shows the progress of the excavation along the longitudinal axis ( $z$ ) and installation of the support by varying the length of a digging step denoted  $d$ . The geometry and the mesh of this tridimensional model is presented by figure 3.b.

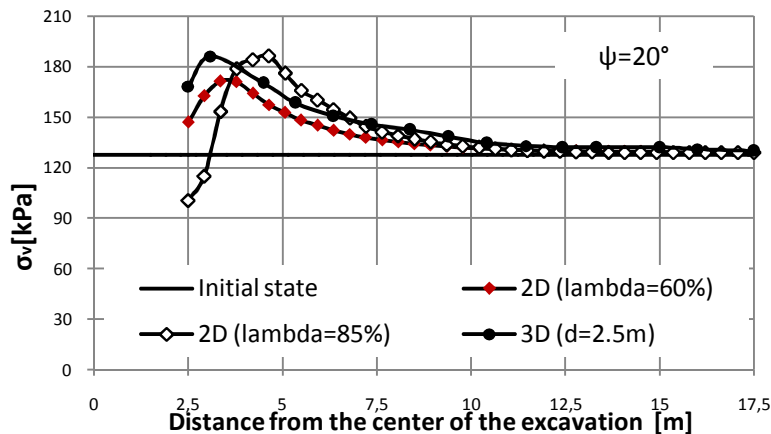


Figure 4. Vertical stress in the soil at 6.5 m of depth of 6.5 m in 3D and 2D ( $\lambda = 85, 60\%$ )

The stress states obtained with 3D and 2D simulations in the ground at 6.5 m of depth at the mid height of abutment are shown in figure 4. We note that the stresses obtained by the 3D model ( $d = 2.5$  m) and 2D model with 85% confinement loss factor are similar. The maximum stress achieved in both cases is in the order of 187 kPa. In terms of plastic zone radius, the evolution reached by bidimensional model with a 60% confinement loss factor is more similar to the tridimensional model than the bidimensional model with 85% confinement loss factor.

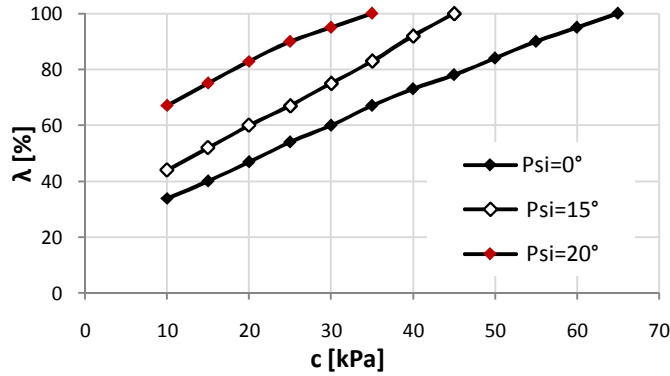


Figure 5. Confinement loss factor as a function of cohesion ( $c$ ) and  $\psi$  ( $\varphi=30^\circ$ )

The numerical simulations, performed with the properties given in Table 1, show that the initial stress state corresponds to 85% confinement loss factor. This state depends on soil properties ( $c$ ,  $\varphi$ ,  $\psi$ ). Figure 5 shows the change in the confinement loss factor in terms of cohesion and dilatancy angle ( $\varphi = 30^\circ$ ). The confinement loss factor  $\lambda$  is proportional to  $c$  and  $\psi$ .

#### Influence of soil properties

Several numerical simulations were performed to study the effect of soil strength properties  $c$  and  $\varphi$ . We present below the results, obtained through this study, in stress curves (Figures 6 and 7) and deformed mesh of axial plastic strain (Figures 8 and 9).

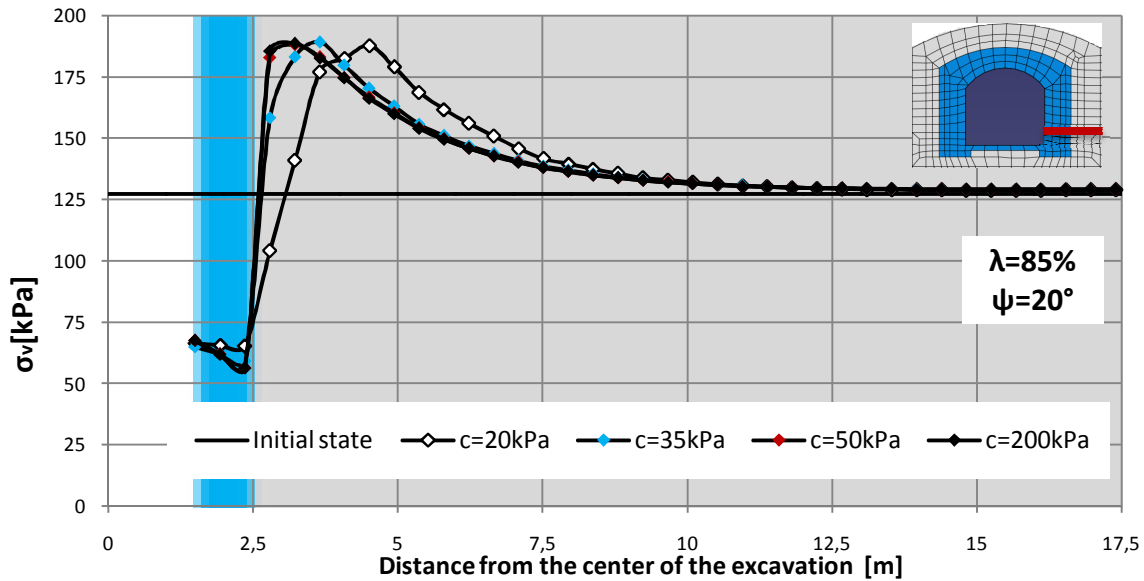


Figure 6. Vertical stress as a function of the distance from the center of the excavation at 6.5m of depth for different values of cohesion

It can be noted that cohesion influences the extension of the plastic zone radius. An increase in the plasticized zone is noted as the cohesion decreases (figures 6 and 8). Beyond 50 kPa of cohesion the initial stress state is the same and plastic deformations are zero. The same trend is observed when considering the friction angle effect (figures 7 and 9): the plasticized zone increases with decreasing  $\varphi$ . The maximum stress values around the masonry support vary according to the friction angle. However, this variation is slightly greater when we compare it with the cohesion effect.

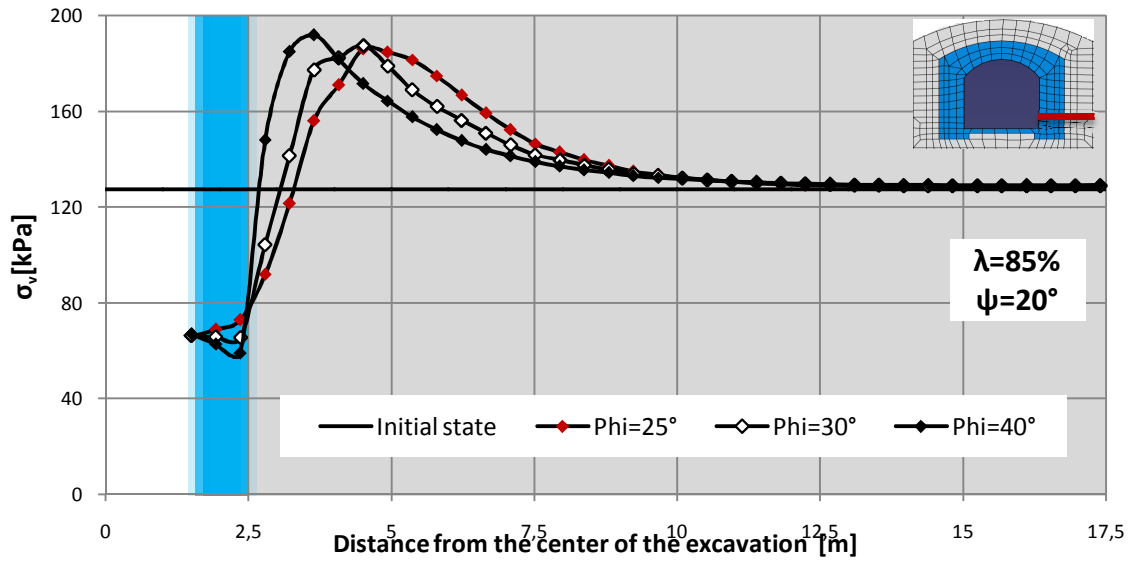


Figure 7. Vertical stress as a function of the distance from the center of the excavation at 6.5m of depth for values of the friction angle

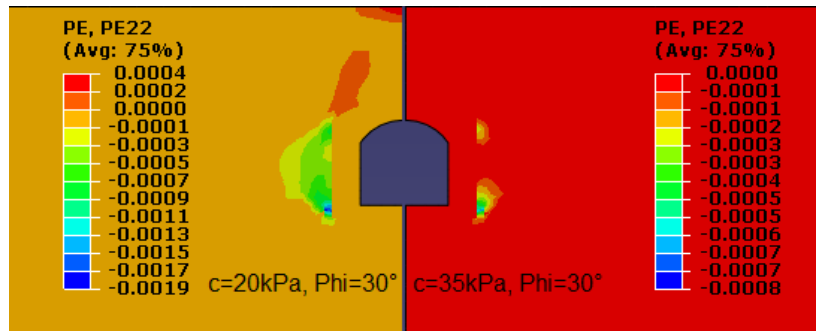


Figure 8. Influence of soil cohesion on the axial plastic deformations ( $\epsilon_{22}$ )

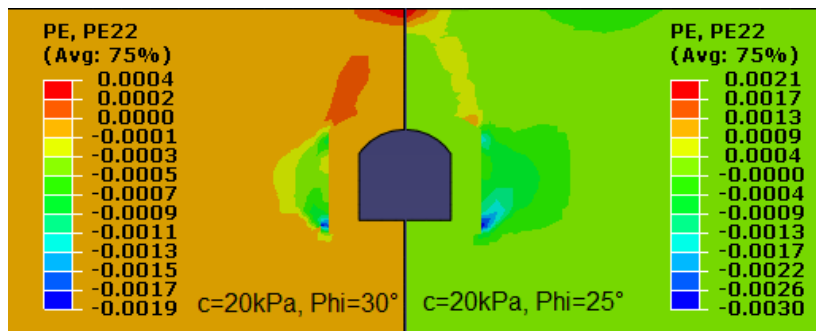


Figure 9. Influence of soil friction angle on the axial plastic deformations ( $\epsilon_{22}$ )

## MODELING OF THE DEGRADED STATE

We remember that among the degradation sources of tunnels of Paris metro, the loss of thrust caused by the deterioration of the old wood shield, or removing of the material constitutive particles due to the water circulation in the ground granular. In following, the degradation is taken into account through two different methods. Firstly, with creation a void between soil and abutment contact. Then, the behavior of masonry lining will be modeled through strain softening law.

### Creation of voids

Because of the occurrence of voids at the contact between the ground and the abutment (deterioration of shielding wood detected by impedance tests), we performed a simulation of the

same gallery taking into account the influence of the void at the abutment which extends over 10 to 20cm (Figure 10).

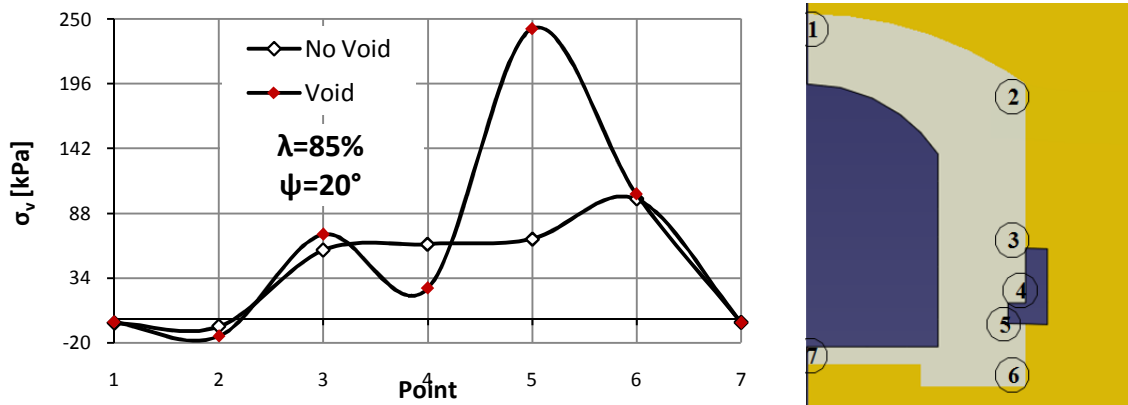


Figure 10. Influence of the void at the abutment on the vertical stresses in the support at different points

The stresses obtained with or without void are the same in points (1, 2, 3, 6 and 7). In point 4, with void model, the vertical stress  $\sigma_v$  decreased by 59% compared to that found without void. The influence of the void is more important in point 5, where the ratio between  $\sigma_v$  (Void) and  $\sigma_v$  (No Void) is above than 3.5. In terms of stress, the influence of the void in point 5 is inverted in relation to the point 4.

Modeling of the gallery with a creation of voids is interesting in the case of location of damaged or cracked areas. With this procedure we could not see the effect of such voids on the global underground structure. For this we proposed to take into account that the mechanical behavior of masonry support is based on a viscoplastic law due to a strain-rate softening as presented in the section below.

#### *Coupling between degradation of cohesion and the creep law*

To simulate the degradation of the masonry lining over time, we use a linear Drucker-Prager criterion with strain softening (Figure 11) coupled with a time hardening law (equation 1). A linear Drucker-Prager criterion was also used with creep law for soil. The physical and mechanical properties of soil and masonry are summarized in table 2.

Table 2. Physical and mechanical properties of soil and masonry

Material	$\rho$ (kg/m <sup>3</sup> )	E (MPa)	$\nu$	d (kPa)	$\beta$ (°)	A (s <sup>-1</sup> )	n	m
Soil	2000	250	0.3	37.5	40.9	3 <sup>e</sup> -14	1	-0.3
Liner1	2400	3200	0.3	173	40.9	1 <sup>e</sup> -16	1.35	-0.5
Liner2				2500		5 <sup>e</sup> -19		

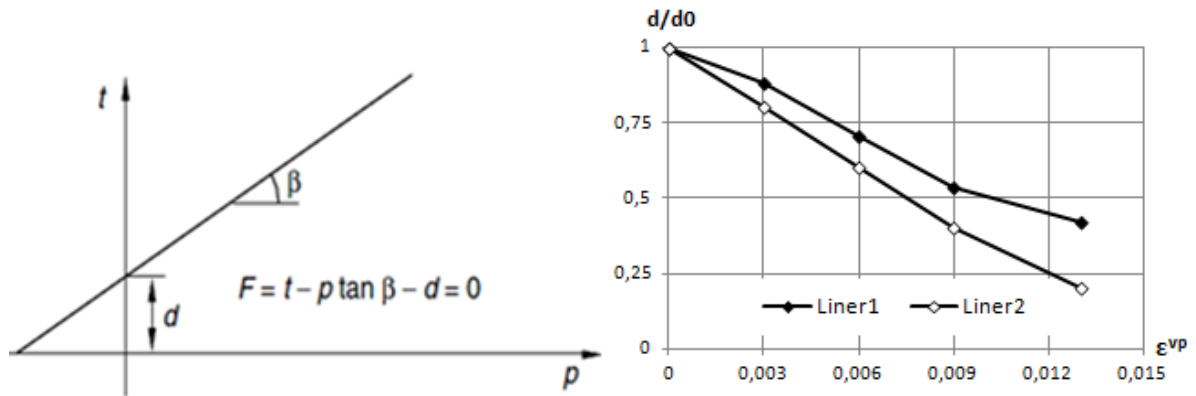


Figure 11. (a): Yield surface of the Drucker-Prager linear criterion, (b): Softening curve of dimensionless cohesion as a function of viscoplastic strain

$$(1) \dot{\epsilon}^{vp} = A(\overline{\sigma}^{cr})^n \overline{t}^m$$

On the figure 11 (a),  $d$  represent cohesion and  $\beta$  the friction angle. The creep model is given by equation 1 and is used to express the rate of plastic deformation  $\dot{\epsilon}^{vp}$ .

$\overline{\sigma}^{cr}$ : present the equivalent creep stress, in our case  $\overline{\sigma}^{cr} = q - p \tan \beta$  because the softening curve is defined by cohesion.  $A$ ,  $n$  and  $m$  are the material parameters (see table 2).

The results of numerical simulation of the behavior of the gallery are shown in Figures 12 and 13. A surface load of 220 kPa is applied over soil surface over 6 m of length.

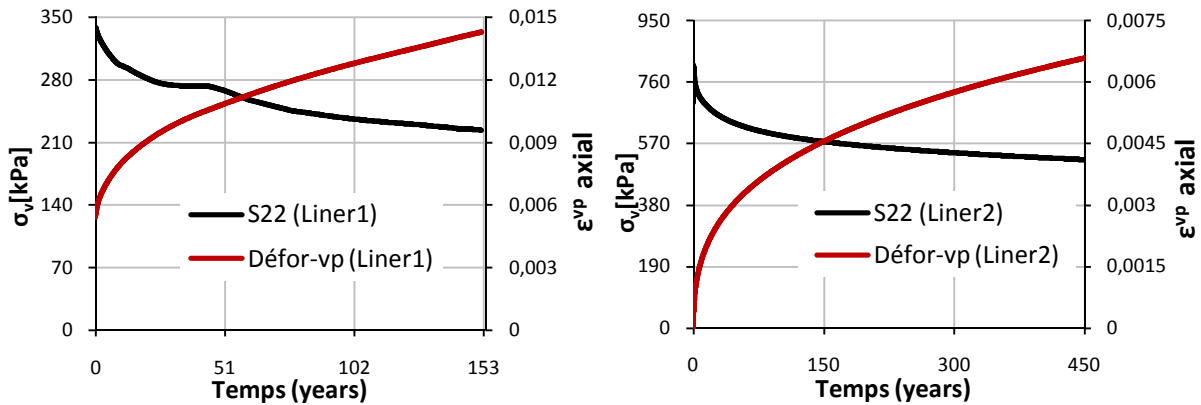


Figure 12. Evolution of inelastic strain and vertical stress in the abutment of tunnel lining (Liner1, Liner2) as a function of time

Stress in Liner 2 is much higher than stress in Liner 1 as shown in figure 12. This difference between stresses is due to the difference between cohesion of Liner 2 and cohesion of Liner 1. Strain softening model allows one to find that the inelastic strain is bigger in Liner1 than in Liner 2. Using this model shows rupture is reached in Liner1 at around 153 years. Whereas, with model Liner 2, stress and inelastic strain progress over time and the rupture is not achieved.

Figure 13 shows horizontal and vertical stress, horizontal and vertical plastic strain at  $t = 0, 100$  and  $153$  years just before collapse; these results are obtained by using strain softening model with Liner1 as masonry lining. The stress  $S_{11}$  and  $S_{22}$  decreases with increasing of plastic strain over time. This figure shows that the compression is concentrated in the abutment and the traction is concentrated in roof which confirms the appearance of cracks in these areas of the metro gallery.



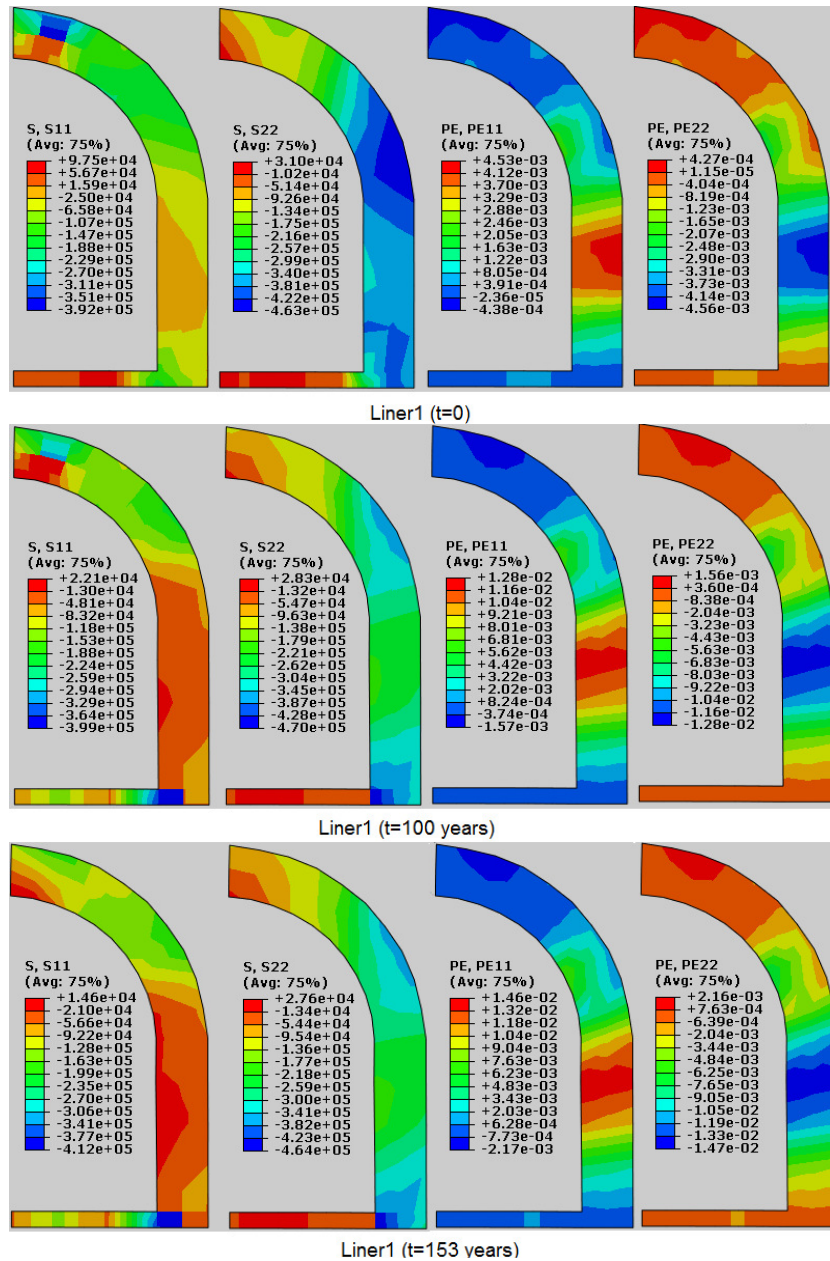


Figure 13. S11: Horizontal stress, S22: Vertical stress, PE11: Horizontal plastic strain, PE22: Vertical plastic strain of Liner1 at t=0, 100 and 153 years. (Sign convention: compression (-), tension (+))

## CONCLUSIONS

The numerical simulation presented in this paper shows that it is possible to reproduce the process of degradation over time of the materials constituting the lining of an underground structure. Strength losses, changes in the stress distribution in the masonry and reveal tension areas in roof which causes cracking. Simultaneously, highly compressed areas appear in the abutment. The application of this approach to other tunnels is planned; however, fine parameters calibration of the constitutive model will be required.

## ACKNOWLEDGEMENTS

This study is as a part of a project devoted to diagnostic methodologies for tunnels and underground structures in operation (MédiTOSS) funded by the French National Agency for Research (ANR).

## REFERENCES

Abaqus. Documentation collection Abaqus/CAE version 6.10.

Boidy E., Bouvard A., Pellet F. (2002), Back analysis of time-dependent behaviour of a test gallery in claystone, *Tunnelling and Underground Space Technology*, Vol. 7 n°4, pp 415-424.

Caquot A., Kerisel J. (1966). *Traité de Mécanique des sols*, Press, Gauthier-Villars (4<sup>e</sup> éd.), pp.444-450.

Fernandez-Merodo J.A., Castellanza R., Mabssout M., Pastor M., Nova R., Parma M. (2007). Coupling transport of chemical species and damage of bonded geomaterials, *Computers and Geotechnics*, Vol. 34, pp. 200-215.

González-Nicieza C., Álvarez-Vigil A.E., Menéndez-Díaz A., González-Palacio C. (2008). Influence of the depth and shape of a tunnel in the application of the convergence-confinement method. *Tunnelling and Underground Space Technology*, Vol.23, pp.25-37.

Idris J., Verdel T., Al-Heib M. (2008). Numerical Modelling and mechanical behaviour analysis of ancient tunnel masonry structures. *Tunnelling and Underground Space Technology*. Vol. 23, pp.251-263.

Idris J., Al-Heib M., Verdel T. (2009). Numerical Modelling of masonry joints degradation in built tunnels. *Tunnelling and Underground Space Technology*. Vol. 24, pp.617-626.

Kasim M., Shakoor A. (1996). An investigation of the relationship between uniaxial compressive strength and degradation for selected rock types, *Engineering Geology*, Vol. 44, pp. 213-227.

Ladanyi B. (1974). Use of the long term strength concept in the determination of ground pressure on tunnel linings, *Proceedings of the Third International Congress on Rock Mechanics*, Vol. IIB, pp. 1150-56.

Ladanyi B. (1980). Direct determination of ground pressure on tunnel linings in a non-linear viscoelastic rock, *Under. Rock Eng. Proceedings of the Thirteenth Canadian Rock Mech. Sym.* Vol. 22, pp. 126-32.

Ladanyi B. and Gill D.E. (1988). Design of tunnel linings in a creeping rock, *International Journal of Mining and Geological Engineering*, Vol. 6, SN:0269-0136, pp. 113-126.

Panet M. (1995). *Le calcul des tunnels par la méthode de convergence-confinement*, Presse. Ecole Nationale des Ponts et Chaussées, pp.125-138.

Pellet F., Hajdu A., Deleruyelle F., Besnus F. (2005). A viscoplastic constitutive model including anisotropic damage for the time dependent mechanical behaviour of rock, *International Journal for Numerical and Analytical Methods in Geomechanics*, Vol. 29 n°9, pp 941-970.

Pellet F., Roosefid M., Deleruyelle F. (2009). On the 3D numerical modelling of the time-dependent development of the Damage Zone around underground galleries during and after excavation, *Tunnelling and Underground Space Technology*, Vol. 24 n°6, SN:0886-7798, pp 665-674.

Pellet F. L. (2009), Contact between a tunnel lining and a damage-susceptible viscoplastic medium, *Computer Modeling in Engineering and Sciences*, Vol. 52 n° 3, pp. 279-296.

Ryu J.-S., Otsuki N., Minagawa H. (2002). Long-term forecast of Ca leaching from mortar and associated degeneration. *Cement and Concrete Research*, Vol. 32, pp. 1539–1544.

Sandrone F., Labiouse V. (2009). Analysis of the evolution of road tunnels equilibrium conditions with a convergence-confinement approach, *Rock Mech. Rock Eng. Vol.* 43, SN: 00603-009-0056, pp.201-218.

Terzaghi K. (1943). *Theoretical soil mechanics*, Press, John Wiley & Sons, pp.190-200.

Torrenti J.M., Nguyen V.H., Colina H., Le Maou F., Benboudjema F., Deleruyelle F. (2008). Coupling between leaching and creep of concrete, *Cement and Concrete Research*, Vol. 38, pp. 816–821.

Wang W. M., Sluys L. J., DE Borst R. (1997). Viscoplasticity for instabilities due to strain softening and strain-rate softening. *International Journal for Numerical Methods in Engineering*, Vol.40, pp. 3839-3864.

Xie S. Y., Shao J. F., Xu W. Y. (2011). Influences of chemical degradation on mechanical behavior of a limestone, *International Journal of Rock Mechanics and Mining Sciences*, Vol. 48, pp. 741–747.